processes

MDPI

Article

Study on Micro-Pressure Drive in the KKM Low-Permeability Reservoir

Heng Zhang [1,*], Mibang Wang [1], Wenqi Ke [1], Xiaolong Li [1], Shengjun Yang [2] and Weihua Zhu [2]

[1] Petroleum Exploration and Production Research Institute, SINOPEC, Beijing 100083, China
[2] International Petroleum Exploration and Production Corporation, SINOPEC, Beijing 100029, China
* Correspondence: zh1216.syky@sinopec.com; Tel.: +86-10-5660-8079

Abstract: Kazakhstan has abundant resources of low-permeability oil reservoirs, among which the KKM low-permeability oil reservoir has geological reserves of 3844 × 10^4 t and a determined recoverable reserve of 1670 × 10^4 t. However, the water flooding efficiency is only 68%, and the recovery efficiency is as low as 32%. The development of the reservoir faces challenges such as water injection difficulties and low oil production from wells. In order to further improve the oil recovery rate of this reservoir, our team developed micro-pressure-driven development technology based on pressure-driven techniques by integrating theories of fluid mechanics and artificial intelligence. We also combined this with subsequent artificial lift schemes, resulting in a complete set of micro-pressure-driven process technology. The predicted results indicate that after implementing micro-pressure-driven techniques, a single well group in the KKM oilfield can achieve a daily oil production increase of 32.08 t, demonstrating a good development effect.

Keywords: low-permeability reservoir; micro-pressure drive development technology; artificial intelligence; artificial lift

check for updates

Citation: Zhang, H.; Wang, M.; Ke, W.; Li, X.; Yang, S.; Zhu, W. Study on Micro-Pressure Drive in the KKM Low-Permeability Reservoir. *Processes* **2024**, *12*, 571. https://doi.org/10.3390/pr12030571

Academic Editor: Carlos Sierra Fernández

Received: 1 February 2024
Revised: 10 March 2024
Accepted: 11 March 2024
Published: 14 March 2024

1. Introduction

During the exploitation of low-permeability reservoirs, due to their characteristics of low porosity, low permeability, and high flow resistance, the field exhibits low production and rapid decline, leading to the existence of a large number of dead oil zones [1,2]. The traditional approach to addressing this issue is hydraulic fracturing, which involves fracturing the near-wellbore formation to generate numerous artificial fractures and improve the flow performance in that area. However, hydraulic fracturing technology is only effective in the short term and often results in severe water flooding due to communication between natural and artificial fractures in the formation [3].

In recent years, a new pressure-driven process has emerged based on hydraulic fracturing technology. The core of the pressure-driven displacement process involves injecting a large amount of water into the formation for a short period at a pressure higher than the formation's fracture pressure. This process forcefully opens natural cracks in the formation and creates a large number of long fractures, thereby improving the flow capacity of injected water and increasing its spread coefficient. However, the disadvantage of this process is that large-scale water injection can easily form preferential channels and cause local "short circuits". In response to the related shortcomings of the pressure-driven displacement process, our team overcame these issues by combining artificial intelligence and plugging technology to develop a micro-pressure-driven displacement process. This process involves finely tuned water injection with a pressure slightly lower than the fracture pressure of the formation, which helps to avoid the formation of preferential channels within the formation. Ultimately, a large number of complex and interlaced three-dimensional networks of micro-fractures are formed.

In 2016, Ding Zupeng and others [4] proposed the optimal fracture aperture limit for water flooding based on their study of the fluid flow characteristics in fractured reservoirs.

The authors analyzed the flow characteristics of micro-fractures and large fractures in a dual-porosity medium. In 2022, Guo Jianchun and others [5] reviewed the progress of tight oil pressure-driven technology in China and divided the process into four stages: Fracturing-Imbibition, Imbibition-Displacement, Fracturing-Energy Storage, Oil displacement-Soaking Well. They also proposed the future direction of pressure-driven development for low-permeability reservoirs, emphasizing the integration of geology and engineering research, and further theoretical research to guide practical application. In the same year, Liu Yikun et al. [6] simulated the pressure-driven process for low-permeability reservoirs using laboratory experiments. The results showed that pressure-driven injection directly into the deep formation has the effect of increasing the sweep efficiency and improving oil recovery. The final increase in recovery is related to the degree of reservoir depletion, with more severe depletion resulting in a larger sweep volume and a more significant improvement in oil recovery. In 2023, Zhang Huali et al. [7] established a CMG numerical model for low-permeability reservoirs and used numerical simulation to optimize pressure-driven parameters, including injection timing, injection volume, and the injection–production ratio. That same year, Xu Dongjin et al. [8] conducted a survey of pressure-driven implementation cases in different areas, such as Shengli Oilfield and Daqing Oilfield in China, summarizing the characteristics of current pressure-driven technology in China. They also analyzed and compared the differences between conventional hydraulic fracturing and pressure-driven technologies and predicted the future development trends of pressure-driven technology.

In 2023, Cui Chuanzhi et al. [9] analyzed the influence of pressure-driven water injection on induced fracture propagation and the impact on injection well pressure from the perspective of crack extension. The study showed that increasing the injection rate leads to more significant crack propagation. In the same year, Sang Congyu and Wang Peng [10], based on an analysis of the pressure-driven mechanism, used numerical simulation to study the impact of extreme permeability contrast and well spacing in the well network on the effectiveness of pressure-driven techniques. The results indicated that cracks, well spacing, and extreme permeability contrast all have a significant impact on pressure-driven technology. Therefore, it is necessary to consider various factors comprehensively in pressure-driven design to ensure the best sweep efficiency and oil displacement efficiency.

In 2023, Cai Xinming et al. [11] conducted a study on the feasibility of pressure-driven processes for low-permeability reservoirs in Jiangsu Oilfield, focusing on the characteristics of low permeability and complex fault blocks in the H59 area. Using numerical simulation techniques, they found that the application of pressure-driven processes in the H59 area can significantly improve well productivity, demonstrating the potential of pressure-driven techniques in low-permeability reservoirs in Jiangsu Oilfield.

In the same year, Yang Yong et al. [12] summarized the understanding of pressure-driven development techniques in Shengli Oilfield, which is known for its abundant low-permeability reservoirs. Since 2020, pressure-driven techniques have been implemented in 450 well groups in Shengli Oilfield. The authors analyzed the adaptability of pressure-driven techniques, the implementation process of on-site pressure-driven operations, and summarized the understanding of pressure-driven processes. They also systematically analyzed the pressure-driven production mechanisms in low-permeability reservoirs in Shengli Oilfield from experimental and numerical modeling perspectives and provided optimization suggestions for future pressure-driven techniques in Shengli Oilfield. These studies have significant implications for the development of low-permeability reservoirs in Shengli Oilfield.

Currently, the development of low-permeability reservoirs is still in the stage of pressure-driven techniques. Pressure-driven techniques have certain positive implications for the development of low-permeability reservoirs. However, pressure-driven techniques require high-pressure injection beyond the formation's fracturing pressure conditions, which makes them prone to channeling. This leads to the formation of numerous preferential pathways underground, where injected water directly enters the wells, limiting the ability to improve the water flooding sweep efficiency.

Building upon pressure-driven technology, our team successfully developed a micro-pressure-driven development technique by integrating the principles of flow mechanics and artificial intelligence (AI). This micro-pressure displacement technique utilizes big data and machine learning methods to analyze formation water injection data and self-learn. It no longer relies on manual experience for adjusting water injection and profile control schemes, but instead employs intelligent-assisted optimization algorithms to achieve precise control of water injection, ultimately creating a large interconnected network of micro-fracture networks within the formation. Taking the KKM oilfield as an example, we established a set of supporting techniques for micro-pressure-driven operations.

The actual process of micro-pressure driving is a long and complex one. Underground conditions are diverse and ever-changing, and pressure control is a key factor. On the one hand, it is necessary to control the injection pressure so that it does not exceed the rock's fracturing pressure. On the other hand, the injection pressure must be as close to the rock's fracturing pressure as possible. Therefore, this process is difficult to control manually and requires the assistance of AI.

First, it is necessary to input the fracturing construction data of other wells in the same area into the AI to allow it to self-learn and understand the fracturing characteristics of different rock formations in the area. When micro-pressure driving begins, only an initial value of micro-fracture pressure of the rock needs to be given to the AI. This value is calculated manually based on the fracturing construction curve. The AI will combine this value with its self-learning results to determine a more accurate range of micro-fracture pressure. Then, instructions are sent to the water injection pump to start micro-pressure driving.

If, at a certain moment during actual injection, the injection process becomes difficult, the AI controller will adaptively increase the injection pressure and provide timely feedback to the water injection pump. Conversely, if the flow rate suddenly increases during water injection, and the concentration of tracer at a certain water well suddenly increases, the AI will immediately make a judgment based on the real-time feedback data from the site to determine whether the formation has been breached. If the AI identifies the presence of a high-permeability channel within the formation, it will immediately instruct the water injection pump to stop micro-pressure driving and instead proceed with sealing the formation.

This process continues iteratively, and eventually, the AI will be able to determine the precise range of micro-pressure driving pressure values based on its learning results and guide the completion of micro-pressure driving work.

2. Material and Methods

2.1. Evaluation of Water Drive Development Effect

The KKM oilfield is located in the Mangystau Region of western Kazakhstan, in the northeastern part of the Caspian Sea. It is approximately 360 km away from the city of Aktau. The field is situated in the central part of the North Ustyurt Basin and covers an oil-bearing area of 64.8 km^2. The oil-bearing formation belongs to the Middle to Upper Jurassic system of the Mesozoic era. The current recovery factor is 20.03%, and the remaining recoverable reserves are estimated to be 887.08×10^4 m^3.

The overall structural configuration of the oilfield is characterized by a long-axis anticline with a near-east–west orientation. The structure is relatively simple, with low amplitude and strong inheritance. Natural fractures are not well-developed, and the reservoir exhibits a transitional marine-continental facies. It is a system that operates under normal temperature and pressure conditions. The reservoir has a porosity ranging from 13.5 to 17.8% and a permeability ranging from 3.1 mD to 14.3 mD, indicating that it is a low-porosity and low-permeability oil reservoir.

Since its inception, the KKM oilfield has been developed using conventional water flooding techniques. Injection pressures have been kept below the formation fracturing pressure. Due to the low porosity and permeability of the reservoir, water injection has been a challenge. Acid fracturing has been employed to enhance the water injection process. However, field experience has shown that acid fracturing is only effective during the first three months, and later on, production can only be maintained through repeated fracturing.

To evaluate the effect of water injection development that has been implemented, we calculated the relationship between the degree of oil recovery and water cut in the oilfield, as well as the relationship between the theoretical and actual changes in water cut for the entire oilfield. We also studied the relationship between the theoretical and actual changes in water saturation over time.

We calculated the relationship between recovery degree and water content, as shown in Formula (1).

$$\lg\frac{f_w}{1-f_w} = 7.5(E_R - \eta) + 1.69 \quad (1)$$

where f_w is the water content of the reservoir, %; η is the recovery rate of the reservoir, %; and E_R is the degree of recovery of the reservoir.

The calculation results of the relationship between oil reservoir recovery degree and water content are shown in Figure 1.

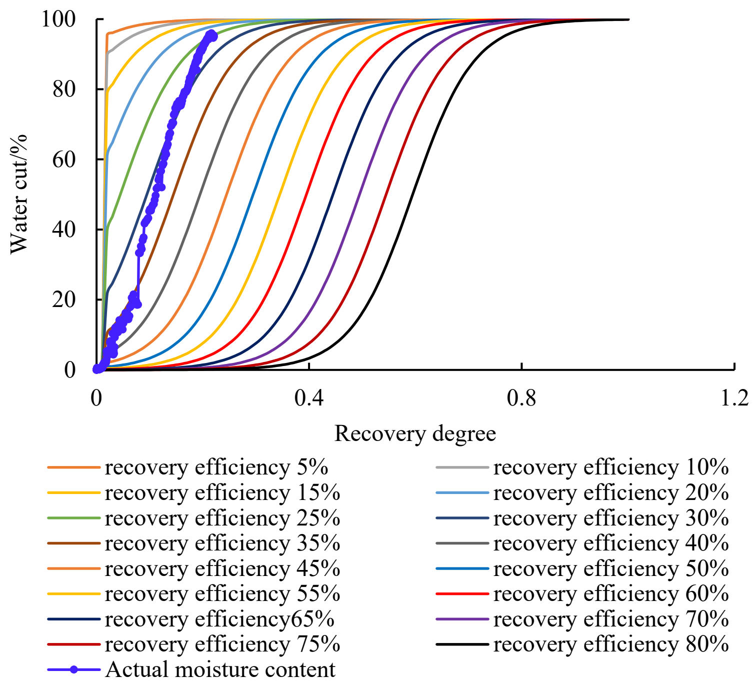

Figure 1. Recovery rate and water content curve.

The calculation of the water cut rise rate curve was performed as follows. Firstly, the actual water cut rise rate was defined as the percentage of water cut increase for every 1% decrease in geological reserves, as shown in Formula (2).

$$m = \frac{f_2 - f_1}{R_2 - R_1} \times 1\% \quad (2)$$

where m is the actual water content increase rate, %; f_1 is the water content in the early stage of mining, %; f_2 is the water content in the late stage of mining, %; R_1 is the degree of extraction in the early stage of mining, %; and R_2 is the degree of extraction in the late stage of mining, %.

The calculation method for the theoretical increase in water content is shown in Formula (3).

$$n = (f_w - f_w{}^2) \times 17.27 \quad (3)$$

where n is the theoretical water content increase rate, %.

The calculation result is shown in Figure 2. Next, we calculated the water storage rate. The calculation method for the actual water storage rate is shown in Formula (4).

$$E_S = \frac{(W_I - W_P)}{W_I} \tag{4}$$

where E_S is the actual water storage rate, %; W_I is the cumulative amount of water injected, m^3; and W_P is the cumulative amount of water produced, m^3.

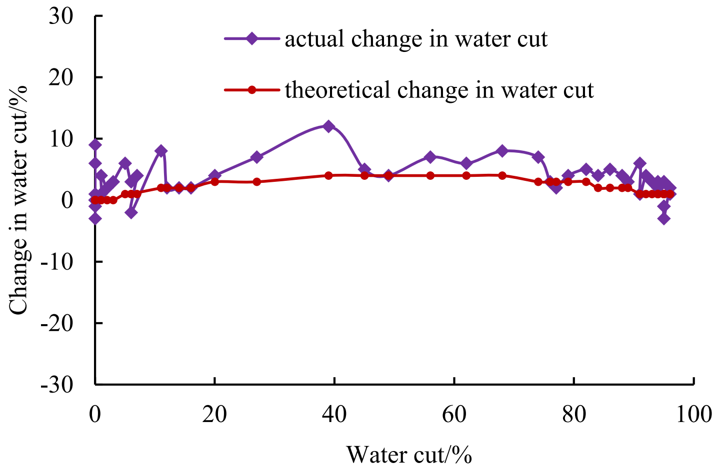

Figure 2. Water content and water rise curve.

The theoretical water storage rate calculation method is shown in Formula (5).

$$E_S\prime = 1 - \frac{f_w}{a \times B_o + a \times (B_o - 1) \times f_w} \tag{5}$$

where $E_S{}'$ is the theoretical water storage rate, %; a is the ratio of the volume of injected water to the volume of produced liquid, dimensionless; and B_O is the volume coefficient of crude oil, dimensionless.

The calculation results are shown in Figure 3.

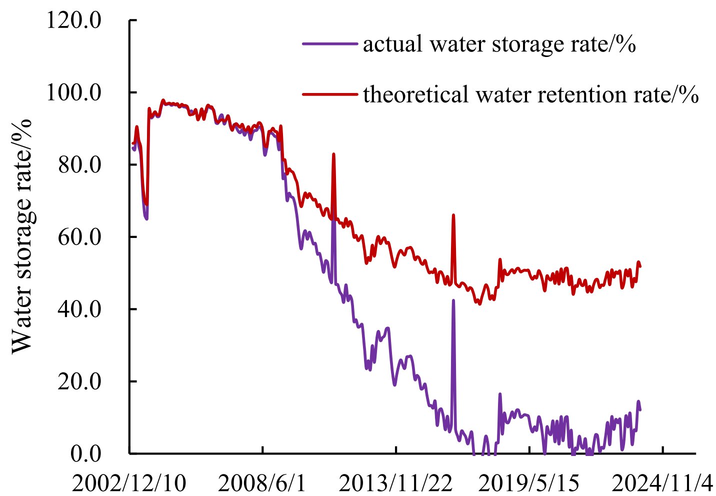

Figure 3. Storage rate variation curve.

From Figure 1, it can be seen that the water cut and oil recovery curve of the KKM oilfield is located in the theoretical curve area of a 30% oil recovery rate, close to the curve of a 25% oil recovery rate, and deviates from the block-calibrated oil recovery rate of 34.9%, indicating that the development situation is gradually getting worse. From Figure 2, it can be seen that the actual water cut increase rate curve fluctuates within the theoretical range, and the overall water cut situation in the oilfield matches the predicted results. From Figure 3, it can be seen that the rate of decline in the oilfield's water storage rate is relatively fast, indicating a decrease in the utilization rate of injected water.

Based on the results in Figures 1–3, currently, the conventional water injection development of the KKM oilfield is becoming less effective, while there is a large amount of remaining recoverable reserves in the field. Therefore, it is necessary to carry out pilot testing of micro-pressure-driven technology. On the one hand, it can supplement the energy of the formation, and on the other hand, it can also improve the injection water sweep efficiency, ultimately improving the oil recovery rate of the reservoir.

2.2. Theoretical Mechanism

In low-permeability reservoirs, there exists a starting pressure gradient in fluid flow, as shown in Figure 4. The fluid at point b begins to flow, which is the minimum starting pressure gradient; point c is the quasi-starting pressure gradient, and point b is the critical pressure gradient. When the reservoir pressure gradient is higher than point d, the fluid in the reservoir truly has fluidity, and the flow law also returns to a straight Darcy flow. When the pressure gradient reaches point a, the flow of micro-pressure displacement truly begins, as there are numerous micro-fracture networks inside the reservoir during micro-pressure displacement. Therefore, the flow of micro-pressure displacement is linear Darcy flow. However, due to the difference between micro-fracture networks and conventional large fractures, there exists a point of initiation pressure gradient in micro-pressure displacement flow, referred to as point a.

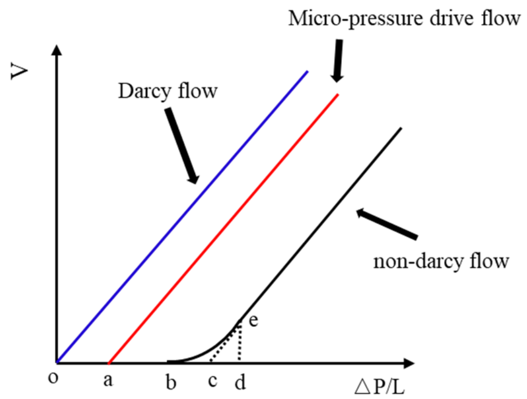

Figure 4. Comparison chart of flow rate curves.

The core concept of micro-pressure displacement flow involves injecting water into the reservoir at or near the rock's micro-fracture pressure, which maintains the formation in a state of micro-cracking. This technique involves the precise sealing of already formed communication fractures and subsequently conducting water injection under micro-fracture pressure followed by repeating the process to form a three-dimensional network of micro-cracks in the reservoir. The fluctuation range of injection pressure and the timing of fracture sealing are intelligently controlled by artificial intelligence software (V1.0).

Specifically, the process involves maintaining the water injection pressure slightly below the formation fracturing pressure while adding oil displacement agents and tracer agents to the injected water. The water injection volume is closely monitored. If the AI software detects a sudden increase in water injection volume at a certain moment and observes a sudden increase in concentration at the wellhead of a particular oil well, the software will automatically analyze the situation. If the software determines that there is a breakthrough channel in the formation and water is rapidly advancing along this channel, it will immediately send a command to stop water injection. Based on the location and concentration of the tracer agent, the software determines the position and volume of the high-permeability channel and promptly injects a sealing agent to block the channel. After the sealing process is completed, fine-tuned water injection is resumed, and the cycle continues until a large number of intertwined and complex micro-crack networks are formed in the reservoir.

By utilizing artificial intelligence algorithms, an piece of intelligent software is developed to automatically control the fluctuation range of water injection pressure and closely monitor the water injection flow rate after the initial determination of the formation's micro-fracture pressure. Additionally, sensors are installed at the wellhead of the water well to promptly transmit tracer agent signals to the intelligent software, enabling intelligent control during the micro-pressure displacement process.

Once a large number of micro-fractures are formed within the formation, the fluid flow within the formation no longer exhibits the curved segments of non-Darcy flow as depicted in points b, c, and d in Figure 4. This is because the complex network of intersecting micro-fractures replaces these segments. The fluid flow within the formation significantly improves due to the presence of these numerous and intricate micro-fractures. However, under such conditions, the flow curve does not follow the straight line passing through the circular point as shown in Figure 4 for Darcy flow. Instead, the actual flow behavior is a linear flow that lies between the two types of flow.

We must clarify that the injection of oil displacement agents during micro-pressure drive is not a necessary factor. The experimental results for oil recovery efficiency in different types of reservoirs are shown in Table 1 and Figure 5. In the figure, "TUO3-8" represents a high-permeability reservoir, while "FAN31," "HE143," and "YI118-8" represent typical low-permeability reservoirs.

Table 1. Comparison of oil displacement efficiency in different types of reservoirs.

Reservoir Type	Well Name	Permeability/10^{-3} μm^2	Oil Displacement Efficiency/%
High-permeability reservoir	TUO3-8	1060	61
Thin interlayer low-permeability reservoir	FAN31	1	58
Lens-shaped rock low-permeability reservoir	HE143	27	60
Thick-layer structural low-permeability reservoir	YI118-8	45	73

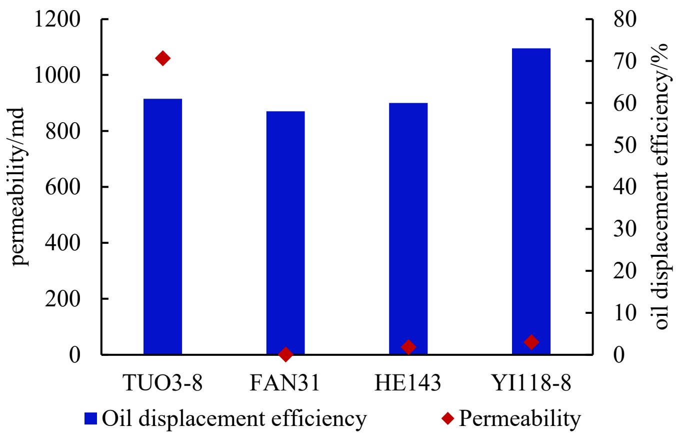

Figure 5. Comparison chart of oil displacement efficiency.

From Figure 5, it can be observed that in low-permeability reservoirs, the areas affected by water injection exhibit oil recovery efficiency comparable to or even higher than that of high-permeability reservoirs. Therefore, for the development of low-permeability reservoirs, the key lies in improving the spreading coefficient of injected water. Whether or not to add oil displacement agents to the water should be determined on site based on budget considerations.

2.3. Theory Comparison

The theory of micro-pressure drive is developed based on the theory of pressure displacement, but they have essential differences. The theory of micro-pressure drive draws on the advantages of pressure displacement while integrating artificial intelligence technology to avoid the drawback of pressure displacement creating high-permeability channels in the formation. Specifically, pressure displacement involves injecting water at a high flow rate above the rock fracture pressure, which quickly replenishes formation energy and enhances well productivity. However, its drawback is the potential formation of high-permeability channels, as shown in Figure 6, where the red part represents high permeability channels. On the other hand, the theory of micro-pressure drive emphasizes injecting water near the micro-fracture pressure of the formation. Through the control of intelligent software, the injection pressure is always kept below the formation fracture pressure, maintaining the formation in a state of micro-fracturing. Precise deep plugging is implemented to seal partially formed communicating fractures. Subsequently, water injection under micro-fracture pressure is repeated in a cyclic manner, ultimately creating a large number of three-dimensional micro-fracture networks within the formation, as illustrated in Figure 7.

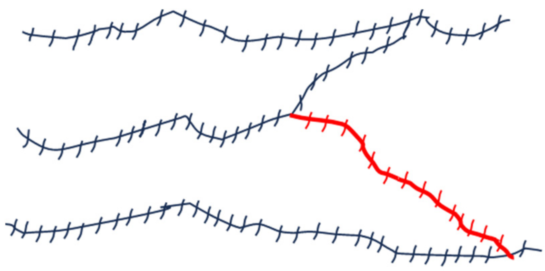

Figure 6. The cracks in pressure-driven processes.

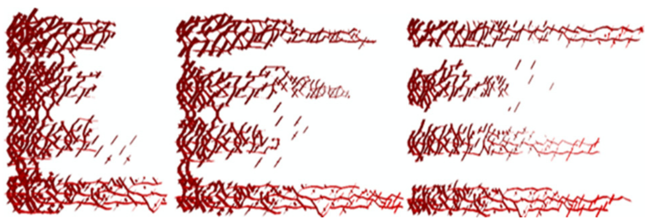

Figure 7. The micro-crack network in micro-pressure-driven processes.

3. Results

We designed a pilot test plan for micro-pressure drive in the KKM oilfield based on the specific conditions of the field. The plan included well and layer selection, engineering design, and follow-up artificial lift plans.

3.1. Well and Layer Selection

Well and layer selection are the basis of micro-pressure drive, and the well selection plan directly affects the final development effect. Therefore, the micro-pressure displacement technology has high requirements for well and layer selection. Specifically, well and layer selection is based on the following factors:

(1) A large distance from the fault to the target layer, and the target layer needs to have a certain thickness and rich remaining oil accumulation in the well group or operating area;

(2) Well groups with well-connected sand bodies and relatively complete injection-production systems;

(3) Reservoirs with poor physical properties, low formation energy, and slow energy recovery rates in segments where injection is ineffective and production is limited;

(4) The surface water injection pipeline is sound, and the water injection wells have high-pressure injection conditions at the wellhead.

The X well group in the KKM oilfield consists of one water injection well (a) and four oil production wells (b, c, d, e), with two primary production wells (b, c) and two secondary production wells (d, e). The geological reserves of the well group are 63.3 × 10^4 t, with cumulative oil production of 14.6 × 10^4 t and a recovery rate of 23.1%. Since production commencement, the total water injection volume is 29.1 × 10^4 m^3 and the cumulative liquid production is 48.1 × 10^4 m^3. The formation pressure drop is 5.7 MPa, with 23.2 × 10^4 m^3 of formation water invasion and a formation deficit of 16.4 × 10^4 m^3, indicating a severe deficit issue.

The well group is connected by sand bodies and is characterized as a barrier island deposition type. The reservoir has a permeability of 10 mD and a porosity of 15%, indicating that it is a low-permeability and -porosity reservoir. Currently, the water injection rate is 20 m^3/d, and there are difficulties in achieving effective water injection.

Based on numerical simulation methods, a study was conducted on the remaining oil reserves in the well group. The results, as shown in Figure 8, indicate that there is abundant remaining oil between the wells in the well group, suggesting a promising production potential. The calculation was carried out using Tnavigator software (V22.1). The product of geological reserves and recovery rate is defined as recoverable reserves. Subtracting the already extracted reserves from the recoverable reserves gives the remaining recoverable reserves.

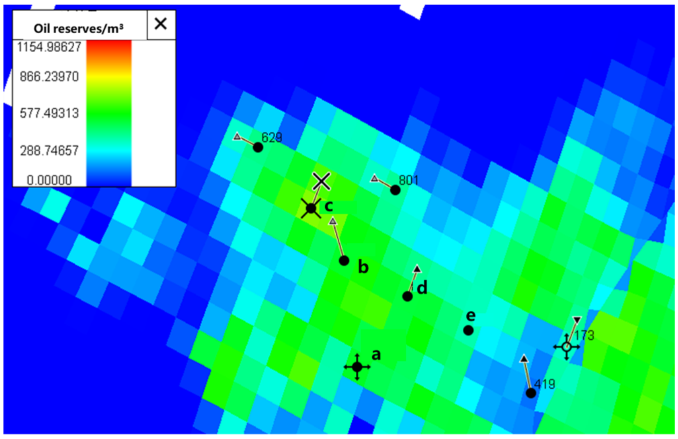

Figure 8. Remaining oil reserves of the reservoir group.

Further calculation of the remaining oil reserves in the well group is shown in Table 2.

Table 2. Remaining oil reserves of the well group.

Original Geological Reserves/10^4 t	Recovery Factor/%	Remaining Oil Geological Reserves/10^4 t	Remaining Recoverable Reserves/10^4 t
63.3	23.1	48.7	4.4

From Table 2, it can be seen that the well group has abundant remaining oil reserves, making it suitable for conducting a pilot test of micro-pressure displacement.

3.2. Scheme Design

To determine the micro-fracturing pressure of the formation, a small-scale fracturing test should be conducted on Well a. The results are shown in Figure 9. Figure 9 shows the actual fracturing construction curve, with the red line representing the variation in wellhead pressure of well a during the fracturing process. The curve exhibits significant fluctuations in the early stages, followed by a rapid increase, and later stabilizes in the region, indicating that there was a brief buildup of pressure in the formation at the beginning of the fracturing process, after which the formation ruptured, and the fractures began to propagate, resulting in a stabilized pressure. From Figure 9, it can be observed that the pressure of the fracturing operation curve initially increases abruptly, then stabilizes, and eventually decreases. By examining a small interval just before the sudden increase in the fracturing operation curve, it can be inferred that the wellhead pressure during micro-fracturing in Well a is between 39 and 40 MPa.

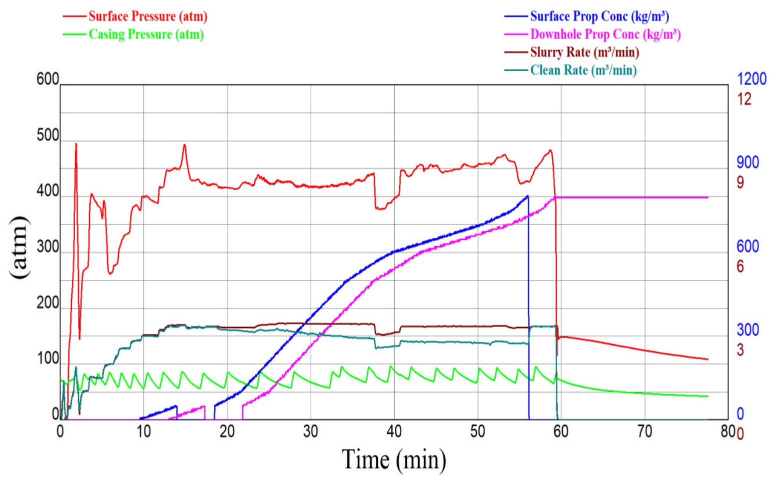

Figure 9. The hydraulic fracturing construction curve for well a.

Therefore, it can be calculated that when micro-fracturing occurs in the formation of Well a, the wellhead pressure is between 39 and 40 MPa. To ensure safety, the calculation was conducted using a maximum wellhead pressure limit of 40 MPa.

Further calculations were conducted to determine the formation pressure during micro-fracturing in Well a, and the results are shown in Figure 10. The calculation was carried out using pipesim software (2017.1).

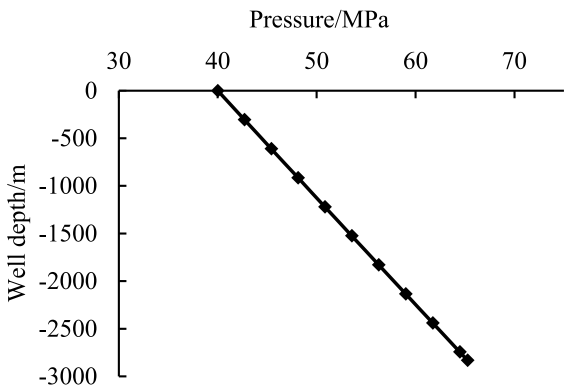

Figure 10. The pressure distribution curve inside wellbore a.

From Figure 10, it can be observed that the formation pressure during micro-fracturing in Well a is 65.25 MPa.

The pressure loss along the 2600 m well depth was calculated, and the results are shown in Figure 11. The calculation was carried out using pipesim software.

From Figure 11, it can be observed that when the inner diameter of the tubing is greater than 62 mm, the pressure loss along the well depth tends to be consistent. Therefore, it can be preliminarily determined that the inner diameter of the water injection tubing for micro-pressure driving is 62 mm.

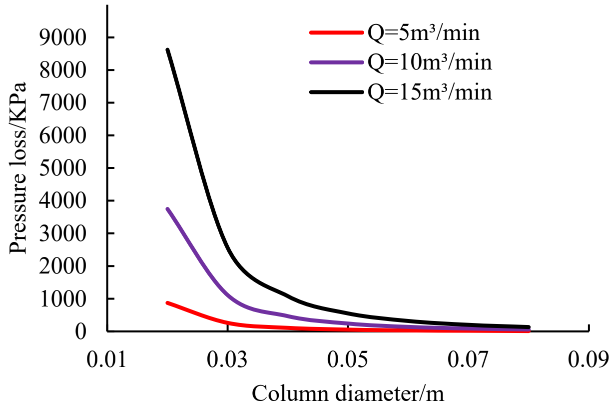

Figure 11. Pressure loss along the wellbore of well a.

Furthermore, we calculated the pressure distribution along the column for different flow rates of a 62 mm pipe, as shown in Figure 12. The calculation was carried out using pipesim software.

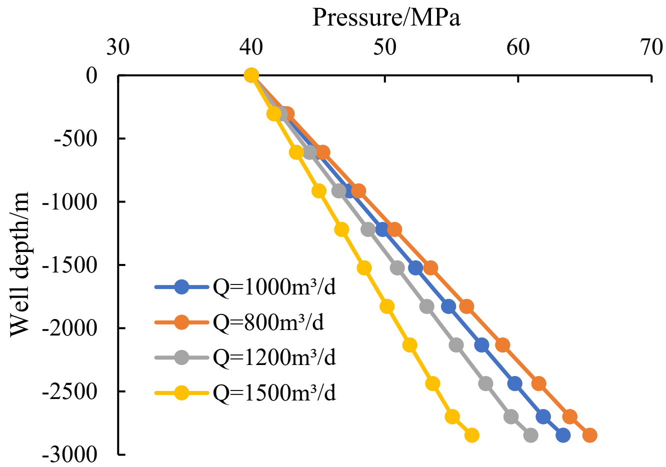

Figure 12. Pressure distribution inside the water injection string with an inner column diameter of 62 mm.

From Figure 12, it can be seen that the greater the flow rate, the greater the pressure loss along the column and the lower the bottomhole pressure. The selection of the pipe material should consider the bottomhole compressive strength under low flow conditions.

On the other hand, when the flow rate is too large, it can cause erosion of the pipe material. Therefore, the selection of the oil tubing size should consider the constraint effect of the erosion flow rate. We calculated the erosion rate for different flow rates and column diameters, as shown in Figures 13 and 14.

The calculation adopted the Hagen–Poiseuille equation.

From Figure 13, it can be seen that the 62 mm inner diameter column has good erosion resistance when the daily injection volume is 500 m^3, but it needs to be replaced when the daily injection volume reaches 800 m^3.

From Figure 14, it can be seen that when the column is replaced with one with an inner diameter of 76 mm, the erosion resistance is significantly improved. This is because the overall principle of micro-pressure drive is to control the injection pressure within the micro-cracking pressure interval without limiting the displacement. Therefore, if the daily injection flow rate reaches 800 m^3, the injection column should be replaced with one with an inner diameter of 76 mm.

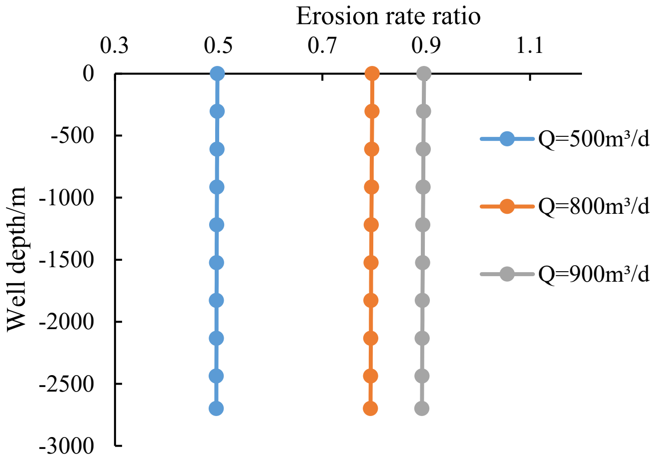

Figure 13. Rate ratio of pipe erosion with an inner column diameter of 62 mm.

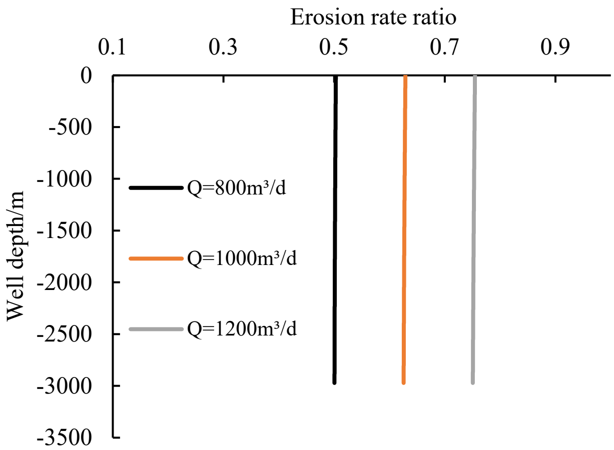

Figure 14. Rate ratio of pipe erosion with an inner column diameter of 76 mm.

After the completion of micro-pressure drive, the formation energy is sufficient, and there will be a short period of self-flow during well opening. After the self-flow stops, it is advisable to use electric submersible pumps for production lifting. After a certain period of production, it is recommended to replace the artificial lifting method with a belt-driven pumping unit to meet the artificial lifting requirements in the KKM oilfield.

4. Discussion

Based on the formation conditions and water influx index of the well group, assuming constant formation pressure, the daily water injection volume of the well group can be predicted under different bottomhole pressure conditions, as shown in Figure 15.

From Figure 15, it can be seen that under the condition of no crossflow channels in the formation, the water injection at the micro-cracking pressure can theoretically predict a daily water injection volume of up to 186 m^3 for the well group.

According to the predicted water injection volume, the relative oil recovery index and relative water recovery index of the well group were calculated by means of reservoir numerical simulation, as shown in Figure 16.

Figure 17 shows a comparison of individual well production rates for the well group at different time periods. From Figures 16 and 17, it can be observed that during the initial production period, the average daily liquid production per well of the well group was 61.7 m^3/d, with a daily oil production of 44.35 m^3/d, water cut of 28.1%, and a relative liquid index of 1.02. Currently, the water cut of the well group has increased to 82%, with a relative liquid index of 1.45. Compared to the initial production period, the liquid index has increased by 1.4 times. Therefore, after the implementation of micro-pressure drive, with sufficient reservoir energy post-implementation, the liquid production can increase to 1.4 times the initial production rate, reaching 86.38 m^3/d. Calculated based on the current 82% water cut, the individual well oil production would be 15.45 m^3/d. This is an increase of 8.02 m^3/d compared to the current individual well oil production of 7.43 m^3/d. With a total of four producing wells in the well group, the overall oil production of the well group would increase by 32.08 m^3/d.

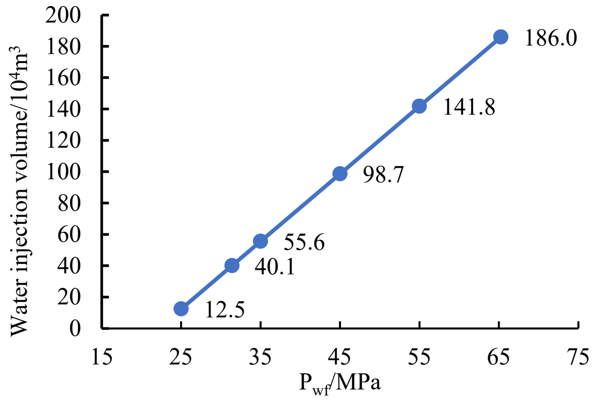

Figure 15. Daily water injection volume of the well group.

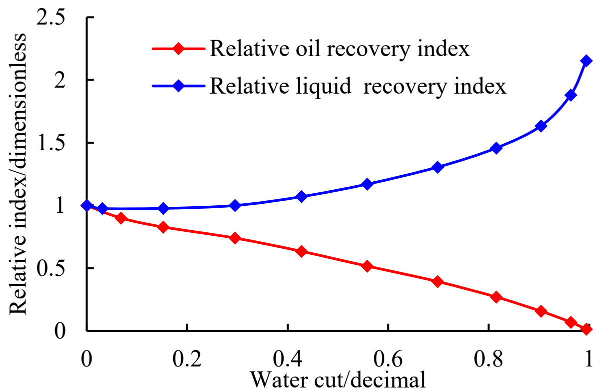

Figure 16. Relative liquid recovery and oil recovery index.

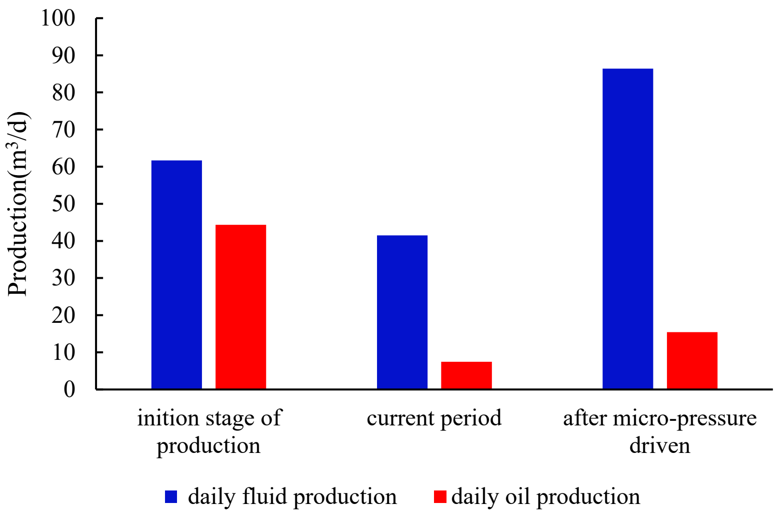

Figure 17. Comparison of production in different periods.

Assuming a production rate of 0.9 during oilfield production and an effective period of 2 years, it can be concluded that the cumulative oil production of the well group can reach 21,076 m^3, indicating very good economic benefits.

5. Conclusions

(1) The KKM oilfield in Kazakhstan has abundant low-permeability reserves but low development utilization, difficulties in water injection well operation, and severe energy deficiency.

(2) Traditional pressure-driven processes are prone to crossflow in the formation. Based on pressure-driven technology, our team has successfully developed micro-pressure-driven development technology by integrating theories of fluid mechanics and artificial intelligence. We have also improved the pilot test plan for micro-pressure-driven techniques, providing a foundation for subsequent artificial lift schemes.

(3) The predicted results indicate that after implementing micro-pressure-driven techniques, a single well group in the KKM oilfield can achieve a daily oil production increase of 32.08 t, demonstrating very promising application prospects.

Author Contributions: Conceptualization, M.W. and W.K.; methodology, H.Z.; validation, X.L., S.Y. and W.Z. All authors have read and agreed to the published version of the manuscript.

Funding: This research was funded by the National Natural Science Foundation of China, grant number U22B6003-01 and SINOPOEC Science and Technology Research Program, grant number P21064-3.

Data Availability Statement: Data are contained within the article.

Conflicts of Interest: Author Heng Zhang, Mibang Wang, Wenqi Ke, Xiaolong Li, Shengjun Yang and Weihua Zhu were employed by the company SINOPEC. The remaining authors declare that the research was conducted in the absence of any commercial or financial relationships that could be construed as a potential conflict of interest.

References

1. Wu, Y.; Shi, L.; Yin, Y.; Qiu, L. Water injection development technology and practice in Liaohe Oilfield. *Spec. Oil Gas Reserv.* **2020**, *27*, 40–46.
2. Kang, Y.; Tian, J.; Luo, P.; You, L.; Liu, X. Technical bottlenecks and development strategies for improving oil recovery in tight oil reservoirs. *Acta Pet. Sin.* **2020**, *41*, 467–477.
3. Mu, L.; Li, X.; Yu, W.; Bu, J.; Li, L.; Liu, T. Research on reasonable ratio of new and old fractures in horizontal wells of ultra low permeability reservoirs after repeated fracturing. *Pet. Drill. Tech.* **2023**, *51*, 97–104.
4. Ding, Z.; Li, N.; Jiao, S. Preliminary exploration of the fracture opening limit for fluid flow in fractured heavy oil reservoirs. *Sci. Technol. Eng.* **2016**, *16*, 122–125.
5. Guo, J.; Ma, L.; Lu, C. Progress and development direction of fracturing and oil displacement technology in tight oil reservoirs in China. *Acta Pet. Sin.* **2022**, *43*, 1788–1797.
6. Liu, Y.; Wang, F.; Wang, Y.; Li, B.; Zhang, D.; Yang, G.; Zhi, J.; Sun, S.; Wang, X.; Deng, Q.; et al. Mechanism of enhanced oil recovery in medium and low permeability reservoir by pressure flooding. *Pet. Explor. Dev.* **2022**, *49*, 752–759. [CrossRef]
7. Zhang, H.; Jin, Z.; Ma, W. Numerical simulation study on pressure drive design in low-permeability reservoirs. *Complex Oil Gas Reserv.* **2023**, *16*, 347–351.
8. Xu, D.; Wu, Y.; Xiong, Q. Current status and development trends of low permeability reservoir pressure drive technology. *Block Oil Gas Fields* **2023**, *41*, 1–16.
9. Cui, C.; Li, H.; Wu, Z.; Zhang, C.; Li, H.; Zhang, Y.; Zheng, W. Analysis of water injection well pressure considering the influence of fractures induced by pressure drive water injection. *Eval. Dev. Oil Gas Reserv.* **2023**, *13*, 686–694.
10. Sang, C.; Wang, P. Research on the influencing factors of pressure flooding effect in low-permeability reservoirs. *J. Beijing Inst. Petro-Chem. Technol.* **2023**, *31*, 27–32.
11. Cai, X.; Huang, Y.; Jin, Z. Research and practice on pressure drive in low permeability reservoirs with complex fault blocks in jiangsu oilfield. *Complex Oil Gas Reserv.* **2023**, *16*, 343–346.
12. Yang, Y.; Wang, J.; Bu, Y.; Zhang, S.; Cao, X.; Lv, Q.; Liu, H.; Yu, C.; Sun, H. Practice and understanding of pressure drive development technology in Shengli Oilfield. *Pet. Geol. Recovery Effic.* **2023**, *30*, 87–93.